

# High- $Q$ polariton modes in heterostructures with traps for dipolar excitons

P.A. Kalinin, V.V. Kocharovskiy, Vl.V. Kocharovskiy

**Abstract.** Polariton modes are studied in two-dimensional traps based on quantum-well heterostructures allowing the production of a Bose–Einstein condensate of indirect excitons. The characteristic equation for the modes is derived using the boundary conditions on the exciton layer located inside a resonator formed by such a trap. The spectrum and the structure of high- $Q$  modes are found analytically and numerically. It is shown that some of these modes become unstable at the high exciton density and long polarisation relaxation time. According to the estimates, this instability can take place in experiments on the Bose condensation of dipolar excitons, thus explaining the origin of their coherent emission.

**Keywords:** polariton modes, Bose–Einstein condensation, dipolar excitons.

## 1. Introduction

Recently, due to extensive investigations of a Bose–Einstein condensation (BEC) in various systems – atomic, molecular, excitonic, the problem of interaction of condensed bosons with the self-consistent electromagnetic field has become urgent. One of the reasons is that in the case of the Bose condensation, the homogeneous and inhomogeneous spectral broadenings of high-frequency oscillations of boson polarisation can be strongly suppressed, which favours the generation of coherent electromagnetic radiation. Of special interest are exciton systems where the condensation can be achieved at temperatures of the order of several kelvins, which is much higher than for atomic and molecular systems [1–6]. In experiments performed with indirect excitons in two-dimensional traps in single and double quantum-well heterostructures (see, for example, [5–19]), the effects indicating the BEC formation were

observed. In particular, exciton luminescence studied in recent experiments [7, 9, 11, 12, 14, 17–19] exhibited interference phenomena, which point to the presence of the spatial coherence of emission of recombining excitons emerging from the trap surface.

In this paper, we study dipolar excitons, i.e. the coupled states of an electron and hole in the external dc electric field, and, thus, having a static dipole moment. Their recombination time ‘is suppressed’ by this field down to several nanoseconds required to thermalise and obtain a rather high density of the excitons being condensed. Nevertheless, they can efficiently interact with the optical electromagnetic field if its frequency is close to that of the exciton recombination. Therefore, in the heterostructures under study, polariton modes can exist, namely, self-consistent polarisation oscillations of excitons and the electromagnetic field. The problem of existence and excitation of polaritons, including excitonic polaritons, in different microresonators was studied by many authors (see, for example, [20, 21]).

In the case under study, a trap accumulating excitons can also serve as a resonator for the electromagnetic field due to the efficient, including total internal, reflection of the latter from a highly conducting heterostructure substrate, surface and side faces of the trap. As a result, certain modes, like whispering gallery modes, can have a high- $Q$  factor. Due to the narrow resonance line of the excitons, one or several such polariton modes can become unstable during the formation of the condensate, and, hence, will be efficiently excited and maintained by induced radiation of new excitons produced by a continuous nonresonance laser pumping, thus producing the coherence of optical dipole oscillations and exciton radiation.

Below, we analyse high- $Q$  polariton modes in such exciton traps taking into account the possible radiative losses and polarisation relaxation but neglecting the exciton dispersion (which is of no importance in the polariton resonance region under study). The corresponding characteristic equation coupling the wave numbers in the directions parallel and perpendicular to the trap plane is studied analytically in the general case and numerically for typical parameters of the experiments [8–12]. It is found that under certain conditions imposed on the exciton density, the relaxation rate of exciton polarisation, and power losses due to radiation from the trap, some modes become unstable. The peculiarities of lasing and resonance scattering of laser radiation as well as the relation between the spectral and polarisation properties of the modes and the parameters of the Bose condensate of dipolar excitons will be studied elsewhere.

P.A. Kalinin, Vl.V. Kocharovskiy Institute of Applied Physics, Russian Academy of Sciences, ul. Ul'yanova 46, 603950 Nizhnii Novgorod, Russia; e-mail: petr@kalinin.nnov.ru, kochar@appl.sci-nnov.ru;  
V.V. Kocharovskiy Institute of Applied Physics, Russian Academy of Sciences, ul. Ul'yanova 46, 603950 Nizhnii Novgorod, Russia; present address: Physics Department, Texas A&M University, College Station, TX 77843-4243, USA

Received 22 December 2008

Kvantovaya Elektronika 39 (11) 1086–1094 (2009)

Translated by I.A. Ulitkin

The problem under study is related to a number of experimental papers [6, 14, 15, 17–19] devoted to the investigation of vertical-cavity surface emitting semiconductor microresonators formed by two Bragg mirrors between which, in the maxima of the mode field of such a resonator, quantum wells filled with excitons are located. The parameters of the microresonators were specially selected so that an electromagnetic mode with the frequency coinciding with the frequency of the exciton transition would exist. In experiments [6, 14, 15, 18, 19], the heterostructures were uniform in the direction along the plane of the quantum wells, and in paper [17], a two-dimensional parabolic trap for excitons was prepared. In all the experiments, the authors observed a drastic increase in the radiation intensity from the structure and the narrowing of its spatial and frequency spectra, when some pump threshold was exceeded, as well as interference phenomena in the emission. In papers [14, 15, 19], the observed phenomena were explained by the Bose stimulation of polariton scattering, which transfers the polaritons to the lower energy state; however, these observations and experiments [7–12] can be explained by the existence and interaction of unstable polariton modes similar to those studied in this paper.

## 2. Trap for excitons as a resonator

For definiteness, we consider a trap with a homogeneous heterostructure used in papers [8–12] (Fig. 1). The structure contains a GaAs quantum well of thickness  $l = 25$  nm in the  $\text{Al}_x\text{Ga}_{1-x}\text{As}$  ( $x \approx 0.33$ ) layer of thickness  $H = 220$  nm. An opaque metal film is deposited on the surface, and directly below the  $\text{Al}_x\text{Ga}_{1-x}\text{As}$  layer there is a highly conducting layer – a highly doped substrate or specially prepared two-dimensional channel with a high mobility and large density of electrons. The distance between the quantum well and the highly conducting substrate is  $h = 50$  nm. In the metal film, holes (circular windows) of diameter  $D = 3 - 10$   $\mu\text{m}$  are etched (the shape of the windows, generally speaking, can be rectangular or triangular). The entire system is exposed to continuous laser

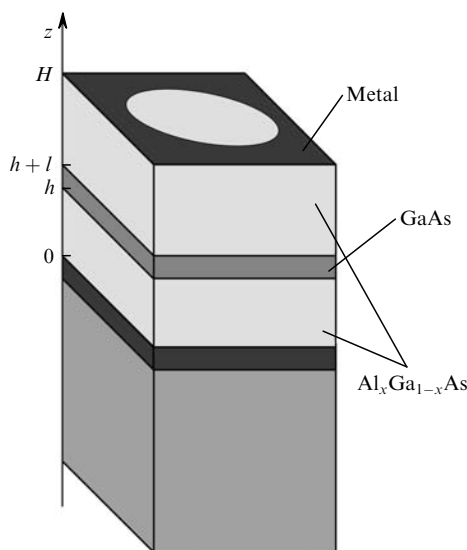


**Figure 1.** Heterostructure with a two-dimensional trap for excitons from paper [9].

pump radiation, which propagates through the mentioned windows and steadily ‘supplies’ electrons and holes to the quantum well, where they are combined into excitons. Between the metal film and a highly conducting layer of the substrate, a dc voltage is applied, which leads to the displacement of the hole and the electron with respect to each other so that the excitons become dipolar and their lifetime  $T_1$  drastically increases (from several nanoseconds to tens of nanoseconds). In this case, the phonons have time to cool the excitons and the density of the latter is maintained by the balance between the pump and recombination at the level sufficient to produce the BEC.

Such a trap can serve as a resonator for the electromagnetic field because the field losses in the highly conducting substrate layer are not high, and under the conditions of grazing incidence, there occurs, in fact, total internal reflection of the wave from the structure surface and substrate. Due to the nonuniformity of the waveguide properties of the heterostructure, there appear reflections from the side faces of the trap (i.e. from the edge of the metal film).

To calculate polariton modes in such a resonator, it is necessary to know the polarisation dynamics of the exciton layer (described by optical Bloch equations), namely, its material equations. The interaction of the exciton with the resonance electromagnetic field proportional to  $\exp(-i\omega t)$  means that the exciton acquires a high-frequency dipole moment under the action of the applied field and when this moment produces a radiation field. Because the exciton layer (quantum well) has a thickness much smaller than other linear dimensions of the problem, we can consider this layer as an infinitely thin resonance dipole layer whose high-frequency component of power (i.e. dipole moment per area unit) is proportional to the applied electric field. We will assume, for simplicity, the nonuniformly broadened emission line of the excitons to be Lorentzian, which, for the linear problem of the mode spectrum investigation and determination of the generation threshold, is tantamount to considering the uniformly broadened line with the effective polarisation relaxation time  $T_2 = (v_2^{(0)} + \Delta v)^{-1}$ , where  $\Delta v$  and  $v_2^{(0)}$  are the nonuniform and uniform line widths, respectively.

In the isotropic case, for the power of the dipole layer formed by the electric field  $\mathbf{E}$  at the frequency  $\omega$ , we have

$$\mathbf{d} = \frac{-\omega_c^2 l}{4\pi} \frac{1}{\omega_0^2 - \omega^2 - 2i\omega/T_2} \mathbf{E}, \quad (1)$$

where

$$\omega_c^2 = 8\pi \frac{|\mathbf{p}_0|^2 N_s \omega_0}{l\hbar} \quad (2)$$

is the square of the so-called cooperative frequency of the medium;  $\omega_0$  and  $\mathbf{p}_0$  are the frequency and dipole moment of the exciton transition;  $l$  is the characteristic thickness of the exciton layer;  $N_s$  is the surface density of the excitons in the well;  $\hbar$  is Planck’s constant.

Allowance for the response anisotropy in expression (1) is reduced to the introduction of different factors for perturbations transverse ( $\eta$ ) and longitudinal ( $\tau$ ) with respect to the layer:  $\omega_{\text{cn},\text{cr}}^2$  and  $T_{2\eta,2\tau}$ . The effective polarisation relaxation time  $T_2$ , which can strongly increase with decreasing the heterostructure temperature [5, 13], is easy to

estimate using the observed spontaneous emission line width of the exciton system. In experiment [9], apart from radiation from the windows, the authors also observed emission from the homogeneous system without windows, in which the metal film on the trap surface was semi-transparent. In both cases, at temperature  $\sim 2$  K, the observed line width corresponded to the energy  $\sim 0.3$  meV, which yields  $T_2 \approx 4$  ps.

The dipole moment value of the exciton transition  $p_0$ , which should be substituted into expression (2), can be found by using the relation of  $p_0$  with the radiative relaxation time  $T_1$  of populations for a two-level system in the medium (heterostructure) with the dielectric constant  $\varepsilon$  [22]:

$$T_1 = \frac{3\hbar c^3}{4\omega_0^3 \sqrt{\varepsilon} |p_0|^2}, \quad (3)$$

where  $c$  is the speed of light in vacuum.

The time  $T_1$ , in fact, is the lifetime of an exciton. In paper [7],  $T_1 \sim 40$  s; in paper [10], this value is several times lower for the conditions of the experiments [8, 9].

Jumps of the electromagnetic field strengths on the dipole layer are found from the boundary conditions, which, taking into account (1), have the form

$$\begin{aligned} E_\tau|_{h-0}^{h+0} &= -2\nabla_\tau(\gamma_n \tilde{E}_n), \\ E_n|_{h-0}^{h+0} &= -2\nabla_\tau(\gamma_\tau \tilde{E}_\tau), \\ H_\tau|_{h-0}^{h+0} &= -\frac{2i\omega\varepsilon}{c} [\gamma_\tau \tilde{E}_\tau, \mathbf{z}_0], \\ H_n|_{h-0}^{h+0} &= 0, \end{aligned} \quad (4)$$

where

$$\gamma_{n,\tau} = \frac{A_{n,\tau}}{\Delta_{n,\tau}}; A_{n,\tau} = -\frac{\omega_{\text{cn},\tau}^2 l}{2\varepsilon}; \Delta_{n,\tau} = \omega_0^2 - \omega^2 - 2i \frac{\omega}{T_{2n,2\tau}}; \quad (5)$$

$$B|_{h-0}^{h+0} = B(z = h + 0) - B(z = h - 0),$$

$$\tilde{B} = [B(z = h + 0) + B(z = h - 0)]/2$$

are the jump and the average value of  $B$  on the layer (difference and half-sum of the values above and below the surface);

$$\nabla_\tau = \nabla - \mathbf{z}_0 \frac{\partial}{\partial z} = \mathbf{x}_0 \frac{\partial}{\partial x} + \mathbf{y}_0 \frac{\partial}{\partial y}$$

is the tangential component of the Hamiltonian (the  $z$  axis is directed along the normal to the layer);  $\mathbf{x}_0$ ,  $\mathbf{y}_0$ , and  $\mathbf{z}_0$  are the coordinate unit vectors;  $\nabla_\tau(\gamma_\tau \tilde{E}_\tau)$  is the two-dimensional divergence. For simplicity, we do not take into account the Lorenz correction to the acting field. This means that in the case of a small jump of the field on the exciton layer [see expressions (17), (18) below], the field affecting the excitons is determined by the average value used above.

Jumps of the fields at the interface of the heterostructure (Fig. 1) with air ( $\varepsilon_1 = 1$ ) at  $z = H$  and with a highly conducting substrate ( $\varepsilon_2 = \varepsilon_2' + i\varepsilon_2''$ ) at  $z = 0$  determine the coefficients of total internal reflection of electromagnetic

waves producing TM and TE modes in accordance with the standard Fresnel formulae [23]:

$$R_{\text{TM}} = \frac{\tilde{\varepsilon}k_n - \varepsilon(\tilde{\varepsilon}k_0^2 - k_\tau^2)^{1/2}}{\tilde{\varepsilon}k_n + \varepsilon(\tilde{\varepsilon}k_0^2 - k_\tau^2)^{1/2}}, \quad R_{\text{TE}} = \frac{k_n - (\tilde{\varepsilon}k_0^2 - k_\tau^2)^{1/2}}{k_n + (\tilde{\varepsilon}k_0^2 - k_\tau^2)^{1/2}}, \quad (6)$$

where  $k_\tau$  and  $k_n = k_n z_0$  are the tangential and normal complex wave vector components of the incident wave;  $\tilde{\varepsilon} = \varepsilon_1$  for the upper boundary and  $\tilde{\varepsilon} = \varepsilon_2$  – for the lower boundary. In the case when  $|k_n| \sim |k_\tau|$  [the thickness  $H$  of the heterostructure is in the order of the wavelength in it  $\lambda = 2\pi c/(\omega_0 \sqrt{\varepsilon})$ ], the highly conducting electronic layer tens of nanometers in thickness (a two-dimensional channel at the interface of GaAs and  $\text{Al}_x\text{Ga}_{1-x}\text{As}$ ) with a large lateral conductivity  $\varepsilon_2''\omega/4\pi \gg 1$  and a real part of the dielectric constant  $\varepsilon_2'$ , which does not differ much from the dielectric constant of the semiconductor  $\varepsilon \approx 13$ , can play the electrodynamic role of the substrate in the resonator. (According to Leontovich boundary conditions, the fields in the substrate will have only tangential components [23], and, correspondingly, the conductivity which can be not so large in the direction perpendicular to the heterostructure layers is not important.)

Because we will be interested in the lower-order transverse modes containing one–two field variations along the  $z$  axis, we can expect for them, according to the theory of nonuniform waveguides, a rather nice reflection of the electromagnetic field from the window boundary, i.e. from the side faces of the trap (we will see below that the reflection coefficient in the order of 0.5 is enough for the mode instability). We will characterise this reflection by one real number – the reflection coefficient modulus in the wave field amplitude  $R_s$ ; the phase of the reflection coefficient does not play an important role because the trap diameter is much greater than the wavelength. Nonideal reflection from the side faces of the trap specifies the nonzero imaginary part of the wave number  $\text{Im} k_\tau$ .

For the one-dimensional trap with the reflection coefficient  $R_s$  from its boundaries, the set of the wave numbers is well known – it is  $k_{\tau m} = \pi m/L + i(\ln R_s)/L$ , where  $L$  is the trap length and  $m$  is the number of the longitudinal mode. In the case of the two-dimensional trap, we will also assume in the estimates that

$$\text{Im} k_\tau = \frac{\ln R_s}{D} = -\frac{|\ln R_s|}{D}, \quad (7)$$

where  $D$  is the trap diameter. Below, it will be also convenient to introduce the effective conductivity  $\sigma$  of the heterostructure, which would give the same value of the imaginary part of wave vector (7) under assumption of an ideal reflection of the waves from the side faces of the trap:

$$\sigma = \frac{c^2 \text{Re} k_\tau}{2\pi\omega} \frac{|\ln R_s|}{D}. \quad (8)$$

(The intrinsic volume conductivity of the used semiconductor structures is small and can be neglected as the imaginary part of the volume dielectric constant proportional to it.)

We will consider the real part of the wave vector  $\text{Re} k_\tau$  as a continuous quantity because at  $D \gg \lambda$  its discreteness plays no significant role for the estimate of the  $Q$  factor and the instability threshold of polariton modes. In addition, for

simplicity, we will assume the density of the excitons to be uniform along the entire plane of the trap, and, hence, we will assume both real and imaginary parts of the tangential wave numbers of all partial waves forming a specific mode of the trap resonator to be identical. In this case, the estimate of the  $Q$  factor and the threshold of the mode instability will be independent of its configuration in the plane of the trap and of the window shape in the metal film at the given (to be calculated) effective reflection coefficient  $R_s$ , which can differ for modes of different configurations, for example Fabry–Perot resonator modes or whispering gallery modes. The peculiarities of laser generation of high- $Q$  polariton modes with a different spatial structure and the effect of their interaction, including with lower- $Q$  modes, for various shapes of the windows in the metal film will be analysed elsewhere.

### 3. Characteristic equations

Taking into account the Lorentzian type of the dipole layer response (1), we will find the resonator eigenmodes by factorising the dependence of the electromagnetic fields on the coordinates in the trap plane and in the direction perpendicular to this plane. According to the aforesaid, we will characterise the modes by the frequency  $\omega$ , the wave number  $k_n$  in the direction perpendicular to the plane of the quantum well, and by the wave number  $k_\tau$  in the plane of the quantum wave.

Because the excitons reside in a very thin layer, they do not affect the mode dispersion equation, which takes the standard form:

$$k_n^2 + k_\tau^2 = \frac{\omega^2 \varepsilon}{c^2}, \quad (9)$$

where  $\varepsilon \approx 13$ . By setting boundary conditions (4) on the layer, we take into account the presence of a quantum well with excitons. Therefore, the parameters of the exciton layer will enter the characteristic equation, which is responsible for the discretization of the  $k_n$  values, and follows from the boundary conditions on the substrate, the trap surface, and the exciton layer. Note that the tangential wave numbers  $k_\tau$ , and, hence, according to (9), the transverse wave numbers  $k_n$  coincide for this mode above and below the exciton layer.

We will take into account the boundary conditions on the highly conducting substrate and on the trap surface by introducing the Fresnel reflection coefficients  $R_b$  and  $R$  with the corresponding phases  $\varphi_b = -i(\ln R_b)/2$  and  $\varphi = i(\ln R)/2 - k_n H$ . In the general case, all these quantities are complex, and different for TE and TM modes; then,  $|R_b| < 1$  and  $|R| < 1$ . When the condition of total internal reflection on the trap surface, which for real wave numbers has the form

$$k_n < k_\tau(\varepsilon - 1)^{1/2}, \quad (10)$$

is fulfilled, the modulus of the reflection coefficient  $R$  will be equal to unity. However, taking into account the mode energy loss, the wave numbers, in the general case, are not real, and, hence, reflection from the surface will not be total although, as shown below, the parameters of high- $Q$  modes will lie in the region

$$\text{Re } k_n < \text{Re } k_\tau(\varepsilon - 1)^{1/2}. \quad (11)$$

The latter inequality is the approximate conditions of reflection that is close to the total one. As for reflection from the substrate, at rather large  $|\varepsilon_2|$ , it will be also almost total. Note that we interested in the vicinity of the mode instability threshold, where  $\text{Im } \omega \approx 0$  and the imaginary part of the transverse wave number is given by the relation

$$\text{Im } k_n \approx -\text{Im } k_\tau \frac{\text{Re } k_\tau}{\text{Re } k_n}, \quad (12)$$

which follows from equation (9).

We will consider first TM modes for which  $H_n = 0$ . The characteristic equation for them has the form

$$\begin{aligned} & 2\gamma_\tau k_n^2 \sin(k_n h + \varphi_{\text{bTM}}) \sin(k_n h + \varphi_{\text{TM}}) \\ & + 2\gamma_n k_\tau^2 \cos(k_n h + \varphi_{\text{bTM}}) \cos(k_n h + \varphi_{\text{TM}}) \\ & + k_n(\gamma_n \gamma_\tau k_\tau^2 - 1) \sin(\varphi_{\text{TM}} - \varphi_{\text{bTM}}) = 0, \end{aligned} \quad (13)$$

where  $\gamma_{n,\tau}$  are functions (5) depending on the complex frequency  $\omega$ . This equation is derived from the condition for the existence of nonzero solutions for the electromagnetic field, these solutions satisfying the boundary conditions on the substrate, surface, and dipole layer. In deriving the equation, we can express all the fields via the Hertz vectors [23] or directly via the tangential component of the magnetic field.

Equation (13) together with dispersion equation (9) determines the curve in the space of three complex quantities  $(k_n, k_\tau, \omega)$ . In particular, by using the specified  $k_\tau$  we can find  $k_n$  and  $\omega$  from these two equations, i.e. all the spectral parameters of the mode. At the points, where the resonance denominator  $\Delta_{n,\tau}$  vanishes [see (5)], the left-hand side of equation (13) is infinite; therefore, it is convenient to multiply this denominator by  $\Delta_n \Delta_\tau$ , thus obtaining

$$\begin{aligned} & 2A_\tau \Delta_n k_n^2 \sin(k_n h + \varphi_{\text{bTM}}) \sin(k_n h + \varphi_{\text{TM}}) \\ & + 2A_n \Delta_\tau k_\tau^2 \cos(k_n h + \varphi_{\text{bTM}}) \cos(k_n h + \varphi_{\text{TM}}) \\ & + k_n(A_n A_\tau k_\tau^2 - \Delta_n \Delta_\tau) \sin(\varphi_{\text{TM}} - \varphi_{\text{bTM}}) = 0. \end{aligned} \quad (14)$$

Note that at  $A_{n,\tau} \rightarrow 0$ , i.e. in the limit of the small exciton density, equation (14) takes the form

$$\Delta_n \Delta_\tau \sin(\varphi_{\text{TM}} - \varphi_{\text{bTM}}) = 0,$$

decomposing into three equations corresponding, obviously, to two partial oscillations of the excitons [tangential ( $\Delta_\tau = 0$ ) and normal ( $\Delta_n = 0$ )] and purely electromagnetic oscillations [ $(\sin(\varphi_{\text{TM}} - \varphi_{\text{bTM}}) = 0)$ ]. In the general case, equation (14) describes three normal modes, which are a superposition of two exciton and one electromagnetic modes. In the case of isotropic polarisation relaxation ( $\Delta_n = \Delta_\tau = \Delta$ ,  $A_n = A_\tau = A$ ) at  $A^2 k_\tau^2 \ll |\Delta|^2$ , the quantity  $A_n A_\tau k_\tau^2$  in the last term can be neglected; as a result, the equation  $\Delta \approx A k_\tau$  describing a purely exciton branch is separated, and we have only the equation describing two electromagnetic-exciton, i.e. polariton, branches. The latter

equation, after substituting into it  $k_\tau^2$  from dispersion equation (9), allows one, in fact, to express the frequency  $\omega$  via the transverse wave number  $k_n$ .

Similarly, we find TE modes for which  $E_n = 0$ . The characteristic equation for them takes the form

$$2\gamma_\tau(k_\tau^2 + k_n^2) \cos(k_n h + \varphi_{TE}) \sin(k_n h + \varphi_{bTE}) - k_n \cos(\varphi_{TE} - \varphi_{bTE}) = 0. \quad (15)$$

As could be expected, the quantity  $\gamma_n$  did not enter this equation because TE modes do not excite exciton oscillations transverse with respect to the layer. Similarly, by multiplying equation (15) by  $A_\tau$ , we obtain

$$2A_\tau(k_\tau^2 + k_n^2) \cos(k_n h + \varphi_{TE}) \sin(k_n h + \varphi_{bTE}) - A_\tau k_n \cos(\varphi_{TE} - \varphi_{bTE}) = 0, \quad (16)$$

and after substituting  $k_\tau^2$  from dispersion equation (9), we obtain the explicit dependence of  $\omega$  on  $k_n$ .

Equation (16) at a small exciton density ( $A_\tau \rightarrow 0$ ) is transformed into the equation

$$A_\tau \cos(\varphi_{TE} - \varphi_{bTE}) = 0,$$

i.e. it is decomposed into the exciton ( $A_\tau = 0$ ) and electromagnetic [ $\cos(\varphi_{TE} - \varphi_{bTE}) = 0$ ] branches and, in the general case, gives a superposition of one exciton and one electromagnetic branches, i.e. two polariton branches.

#### 4. Mode spectrum: numerical calculation

In the general case, to calculate the mode spectrum, i.e. to search for the dependences  $\omega(k_\tau)$  and  $k_n(k_\tau)$ , it is necessary to solve numerically the systems of dispersion (9) and characteristic (13), (15) equations, which is convenient to do in stages. First, we can find the real spectrum in the absence of losses by calculating the left-hand side of the characteristic equation for discrete, closely spaced values of  $k_n$  and  $k_\tau$  and their corresponding frequency  $\omega$  from the dispersion equation; after that, we separate the regions, where the left-hand side of the equation changes its sign, and define the solution by the binary search method. Then, the complex spectrum (taking into account the losses) is found by the Newton method using, as an initial approximation, the system of solutions obtained from the real equation and exact partial solutions obtained in the absence of interaction between the excitons and the electromagnetic field.

We will use the typical parameters of the experimental setup [9]:  $\varepsilon = 13$ ,  $H = 220$  nm,  $h = 50$  nm,  $l = 10$  nm,  $\omega_0 = 2.3 \times 10^{15}$  s $^{-1}$  (the exciton energy,  $\hbar\omega_0 = 1.5$  eV; the wavelength in the heterostructure,  $\lambda \approx 220$  nm =  $H$ ), the trap diameter  $D = 5$   $\mu$ m. For definiteness, we will present all the calculations for the isotropic case ( $\gamma_n = \gamma_\tau = \gamma$ ,  $A_n = A_\tau = A$ , etc.). For simplicity, we will restrict ourselves to the case of ideal reflection for the highly conducting substrate:  $|R_b| = 1$ ; below we will ascertain the conditions under which this approximation can be used. Note that the selected parameters at the reflection coefficients from the side faces of the trap  $R_s \sim 0.5$  correspond to the effective conductivity of the heterostructure (8), which is much greater than the inverse time of the polarisation relaxation

( $\sigma \gg 1/T_2$ ), i.e. to class D lasers [24, 25] in which polarisation of the excitons lives longer than that of phonons and generation is caused by the polariton and not by the electromagnetic mode.

With these parameters there exist two intersection regions of unperturbed electromagnetic and exciton branches of the spectrum for TM modes and two more regions for TE modes corresponding to TM<sub>0</sub>, TM<sub>1</sub>, TE<sub>0</sub>, and TE<sub>1</sub> modes of this planar waveguide. Their transverse wave numbers satisfy the conditions  $k_n H \approx \pi/2$  (TM<sub>0</sub>),  $\pi$  (TE<sub>0</sub>),  $3\pi/2$  (TM<sub>1</sub>), and  $2\pi$  (TE<sub>1</sub>) [exact equalities would take place at  $R_{TM,TE} = -1$ , which is valid at  $k_\tau(\varepsilon - 1)^{1/2} \gg k_n$ ].

Typical complex spectra of polariton TM<sub>0</sub> modes are presented in Fig. 2 for the surface density of the excitons  $N_s = 10^{11}$  and  $10^{10}$  cm $^{-2}$ ; in this case, the cooperative frequency  $\omega_c$  was calculated using (2) where we substituted the dipole moment (related to the electron charge)  $p_0/e \approx 3$  Å found [see (3)] with the help of the radial decay time of the excitons  $T_1$ , which, for definiteness, was taken equal to 2 ns (in accordance with [10]). As was shown above, the polarisation relaxation time is  $T_2 = 4$  ps, and the reflection coefficient from the side faces of the trap is  $R_s = 0.8$ . One can clearly see that at the given parameters, the branches are not ‘overlapped’, i.e. in the case of continuous motion along the branch, the jumps are absent: there exist two exciton branches (those, which merge far from the intersection region) and one electromagnetic branch.

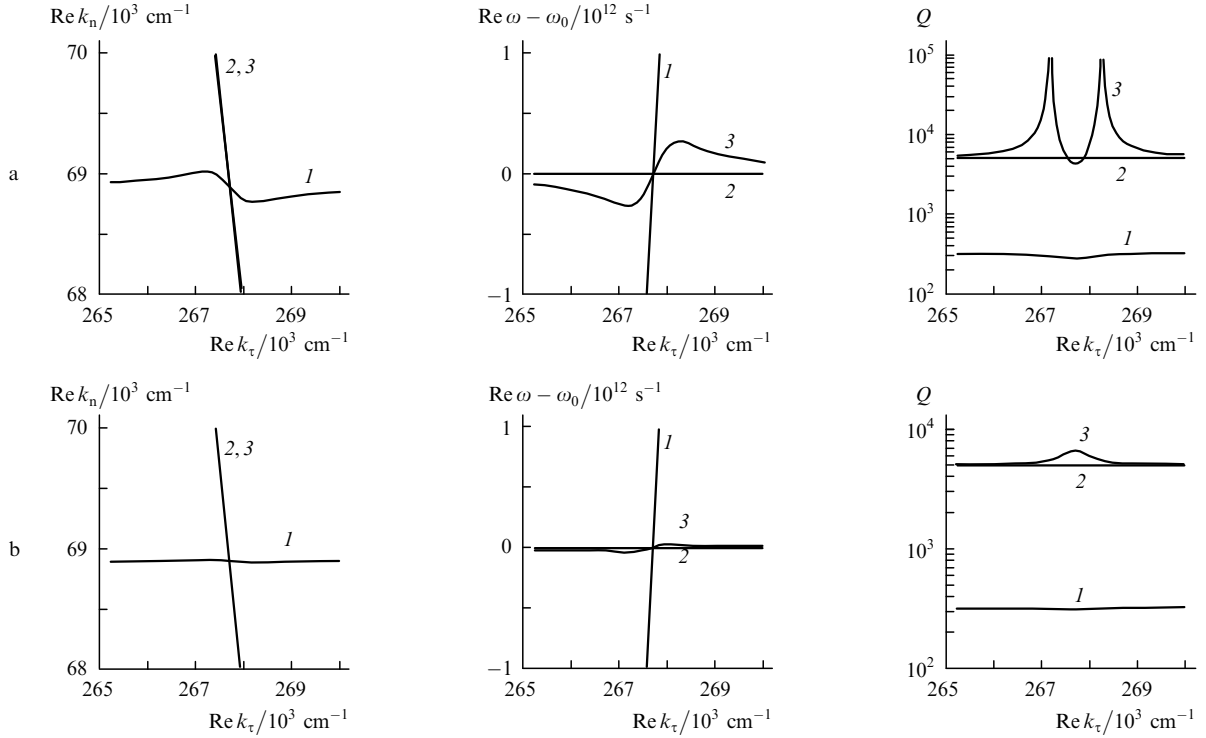
At  $N_s = 10^{10}$  cm $^{-2}$  (Fig. 2b), the mode spectrum insignificantly differs from the unperturbed one, while at  $N_s = 10^{11}$  cm $^{-2}$  (Fig. 2a), some TM<sub>0</sub> modes near the resonance ( $k_n^2 + k_\tau^2 = \omega_0^2 \varepsilon / c^2$ ) become unstable ( $\text{Im } \omega > 0$ ). The latter is evidenced by the presence of two singularities on the exciton (polariton) branch of the dependence of  $Q = |\text{Re } \omega / (2\text{Im } \omega)|$  on  $\text{Re } k_\tau$  between which  $\text{Im } \omega > 0$ ; for the electromagnetic branch and the other split exciton branch, the instability is absent, i.e.  $\text{Im } \omega < 0$  everywhere. This is natural for these parameters at which the  $Q$  factor of unperturbed electromagnetic modes is lower than that of unperturbed exciton modes. A higher- $Q$  factor of the electromagnetic modes that would correspond to the electromagnetic branch instability requires close-to-unity values of  $R_s$ , which are hardly realised in the experiments. The presence of the weakly perturbed exciton (third) branch is also natural because under these parameters  $A^2 k_\tau^2 \ll \Delta^2$  for two polariton modes.

Figure 3 shows the field structure of the polariton mode with the largest instability increment at  $N_s = 10^{11}$  cm $^{-2}$ . One can see that the jump of the field (or the field derivative) on the layer can achieve  $\sim 10\%$ . It is easy to obtain from conditions (4) an expression for the relative jumps of the field. For example, for the  $E_\tau$  component we have

$$\frac{E_\tau|_{h=0}^{h+0}}{\bar{E}_\tau} \sim \frac{k_\tau^2}{k_n} \gamma_n. \quad (17)$$

For the modes in the vicinity of the instability threshold [see condition (31) below], we can write the following expression:

$$\frac{E_\tau|_{h=0}^{h+0}}{\bar{E}_\tau} \sim \frac{\pi\sigma}{\varepsilon\omega_0} \frac{k_\tau^2 H}{k_n}. \quad (18)$$



**Figure 2.** Complex spectrum of  $TM_0$  modes consisting of the electromagnetic (1), detached (2), and polariton (3) branches: real parts of the wave numbers  $Re k_n$ , the differences  $Re \omega - \omega_0$ , and the quantities  $Q = |\text{Re} \omega / (2\text{Im} \omega)|$  (equal to the  $Q$  factors for the stable modes and characterising the increment for the unstable modes) as a function of  $Re k_\tau$  at  $N_s = 10^{11}$  (a) and  $10^{10} \text{ cm}^{-2}$  (b).

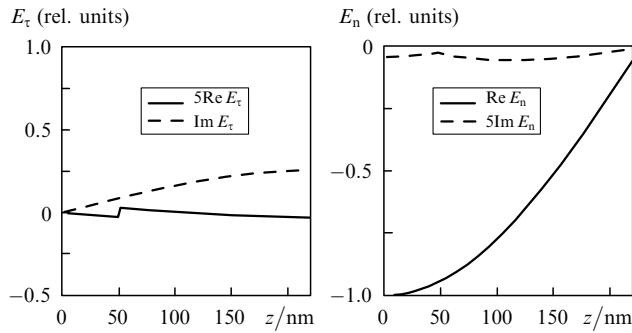


**Figure 3.** Field structure of the  $TM_0$  mode.

One can see from this expression that the jump is not high and is determined, first of all, by the small ratio  $\sigma/\omega_0$ .

The calculation results for the  $TM_1$ ,  $TE_0$ ,  $TE_1$  modes are completely analogous and are not presented in this paper.

It is convenient to study numerically the boundary of the mode instability region on the plane  $N_s, R_s$  by the binary search method with respect to the variable  $R_s$  for each of four intersection regions of the unperturbed electromagnetic and exciton branches by finding the threshold value  $R_s$  at which the instability appears in the centre of each region. The dependences obtained for  $TM_0$ ,  $TM_1$ ,  $TE_0$ , and  $TE_1$  modes are presented in Fig. 4. One can see that the instability of the modes does not require very high reflection coefficients from the side faces of the trap, and the values of  $R_s$  down to 0.5 are sufficient.

## 5. Mode spectrum: analytic solution

The above results can be obtained analytically by solving a system of the characteristic and dispersion equations

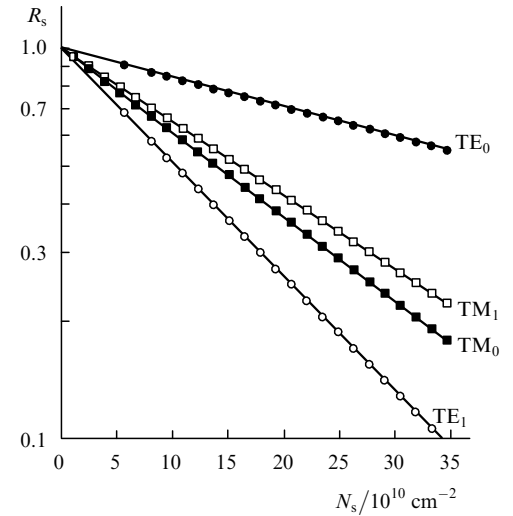


**Figure 4.** Boundaries of the instability region in the plane  $N_s, R_s$ ; laser generation of each mode starts above the straight line corresponding to it.

expanded in series in the vicinity of the resonance and by finding the frequency  $\omega$  as a function of deviation from the resonance value of the real part of the wave number  $Re k_\tau$ , which plays the role of the spectral parameter [the imaginary part of  $k_\tau$  is given by relation (7)]. We will consider only the TE modes; similar results can be easily obtained for TM modes, and if we initially neglect the term  $\gamma_n \gamma_\tau k_\tau^2$  in equation (13), i.e. split almost purely exciton branch, the calculations for the TM modes in the isotropic case virtually coincide with those presented below.

The expansion in series is conveniently performed in the vicinity of the point corresponding to the intersection of

unperturbed real branches, which are obtained in the absence of losses and relaxation. The corresponding wave numbers and the frequency are found from the conditions

$$\begin{aligned}\omega &= \omega_0, \\ k_\tau^2 + k_n^2 &= \frac{\omega^2 \varepsilon}{c^2}, \\ \cos \varphi_{\text{TE}} &= 0.\end{aligned}\quad (19)$$

We will designate below the solution of this system as  $\bar{k}_n$ ,  $\bar{k}_\tau$ , and  $\bar{\omega} \equiv \omega_0$ ; they are all real. Note that the resonance denominator  $\Delta$  for them will be nonzero despite the fact that it is equal to zero for purely exciton modes, taking into account the polarisation relaxation.

The expansion in series can be also performed by taking, as an initial approximation, the parameters corresponding to the intersection point of unperturbed complex branches, which are obtained taking into account the polarisation relaxation of the excitons but by neglecting the emission from the trap. The characteristic feature of this consideration results in the presence of imaginary parts in the unperturbed frequency ( $\text{Im } \bar{\omega} = -1/T_2$ ) and, hence, in the wave numbers  $k_\tau$  and  $k_n$ , is not associated directly with the emission from the trap. The final results are, of course, independent of the decomposition technique and are obtained equal.

Below, it will be convenient to use the notations

$$C_n = \left| \frac{\partial}{\partial k_n} \cos \varphi_{\text{TE}} \right|, \quad \zeta = \cos(\bar{k}_n h + \varphi_{\text{TE}}) \sin(\bar{k}_n h + \varphi_{\text{bTE}})$$

and assess the results taking into account  $\zeta \sim 1$  and

$$C_n = \left| \frac{\partial}{\partial k_n} \cos \left( i \frac{\ln R_{\text{TE}}}{2} - \bar{k}_n H \right) \right| \sim H$$

(the latter estimate is obtained by neglecting the weak dependence of  $R_{\text{TE}}$  on  $k_n$ , which, in particular, describes the possible emission of the modes through the heterostructure surface).

The obtained results can be readily expressed by the effective conductivity  $\sigma$  of the medium (8). In this case, it turns out that the absorption of the modes in the substrate enters the final expression as a term, which is added to  $\sigma$ ; therefore, we will introduce an additional effective conductivity of the resonator volume caused by the losses in the substrate:

$$\begin{aligned}\sigma_b &= \frac{c^2 \text{Re } k_n}{2\pi\omega} \frac{\text{Im } \varphi_{\text{bTE}}}{C_n} = \frac{c^2 \text{Re } k_n}{4\pi\omega} \frac{|\ln |R_b||}{C_n} \\ &\sim \frac{c^2 \text{Re } k_n}{4\pi\omega} \frac{|\ln |R_b||}{H}.\end{aligned}\quad (20)$$

Then, the total conductivity

$$\sigma_\Sigma = \sigma + \sigma_b \quad (21)$$

will enter the final expressions. The presence of the multiplier 4 in the denominator of expression (20), unlike the multiplier 2 in the denominator of (8), is explained by the fact that the losses through the side faces occur twice

per transit of light in the resonator and the losses through the substrate – once.

The condition of ideal reflection from the substrate used earlier becomes obvious from the above said: the field absorption in the substrate can be neglected, if  $\sigma \gg \sigma_b$ , i.e. if

$$\frac{k_\tau |\ln R_s|}{D} \gg \frac{k_n |\ln R_b|}{2H}, \quad (22)$$

which, for the above parameters and  $R_s \sim 0.5$ , yields  $R_b > 0.97$  corresponding to very high dielectric constants of the highly conducting substrate layer:  $|\varepsilon_b| \gg 5 \times 10^5$ . In the limit corresponding to inverse inequality (22), we can neglect the emission through the side faces of the trap.

In the notations used in the main order of the perturbation theory, the frequencies of the polariton modes depend on  $\text{Re } k_\tau$  as follows:

$$\begin{aligned}\delta\omega &= -i \frac{1}{2T_2} - i \frac{\pi}{\varepsilon} \sigma_\Sigma + \beta \delta \widetilde{k}_\tau \\ &\pm i \left[ \left( \frac{1}{2T_2} - \frac{\pi}{\varepsilon} \sigma_\Sigma - i \beta \delta \widetilde{k}_\tau \right)^2 + \frac{\omega_c^2 l_\zeta^2}{2\varepsilon C_n} \right]^{1/2}.\end{aligned}\quad (23)$$

Here,  $\delta\omega = \omega - \omega_0$  is the frequency shift of the mode from the frequency of the exciton resonance;  $\beta = c^2 \bar{k}_\tau / (2\varepsilon \omega_0)$ ;  $\delta \widetilde{k}_\tau = \text{Re } k_\tau - k_\tau^{(0)}$ .

The line centre  $k_\tau^{(0)}$ , i.e. the value of the real part of the wave number  $\text{Re } k_\tau$ , at which the maximum of the imaginary part of the frequency (increment maximum or decrement minimum) is achieved, does not coincide with the unperturbed value of  $\bar{k}_\tau$  obtained from conditions (19) but is shifted from it by the quantity

$$k_\tau^{(0)} - \bar{k}_\tau = \frac{\bar{k}_n}{\bar{k}_\tau} \frac{\text{Re } \varphi_{\text{bTE}}}{C_n}. \quad (24)$$

This shift is explained by the fact that when the finite conductivity of the substrate is accounted for, not only the modulus of the reflection coefficient from the substrate [it is taken into account in (20)] but also its phase change, which leads to a shift of the partial electromagnetic branch. Note again that we study the frequency dependence  $\omega$  on the real part of the wave number  $k_\tau$ , which determines the specific mode.

The real part of the frequency in the line centre proves equal to the frequency  $\omega_0$  of the exciton transition, i.e. the line centre is not shifted from the resonance.

Note that expression (23) can be derived in a different way. Namely, assuming that the field structure of polariton modes will weakly differ from that in the unperturbed electromagnetic mode [see (17), (18), and Fig. 3], we can find their spectrum by using the solution of the known problem of the excitation of the resonator by the given polarisation sources [23]. In this approach, the fields in the resonator will have the form

$$\mathbf{E} = e(t) \mathbf{E}_m(\mathbf{r}), \quad (25)$$

$$\mathbf{H} = h(t) \mathbf{H}_m(\mathbf{r}),$$

where  $\mathbf{E}_m(\mathbf{r})$  and  $\mathbf{H}_m(\mathbf{r})$  are spatial mode structures of the unperturbed resonator, and the excitons will be the polarisation sources exciting the resonator, the polarisation

amplitude being proportional to the electric field of the mode. By substituting fields (25) and the polarisation exciting them in Maxwell's equation, we can easily obtain an equation for the coefficients  $e(t)$  and  $h(t)$ , which leads to the equation for the frequencies of the polariton modes,  $\omega$ :

$$\omega_m^2 - \omega^2 = -\frac{\xi\omega^2\omega_c^2 l}{\varepsilon(\omega_0^2 - \omega^2 - 2i\omega/T_2)}. \quad (26)$$

Here,  $\omega_m$  is the complex frequency of the unperturbed electromagnetic mode and

$$\xi = \frac{\int \mathbf{E}^2 dS}{\int \mathbf{E}^2 dV} \sim \frac{1}{H}, \quad (27)$$

where integration in the numerator is performed over the exciton layer surface and in the denominator – over the entire volume of the resonator.

The imaginary part of the electromagnetic mode frequency  $\text{Im } \omega_m$  is caused by its decay:

$$\text{Im } \omega_m = -\frac{2\pi i \sigma_\Sigma}{\varepsilon}. \quad (28)$$

The difference between the real part of the electromagnetic mode frequency  $\text{Re } \omega_m$  and exciton resonance frequency  $\omega_0$  plays the role of a spectral parameter and can be expressed through the shift  $\delta k_\tau$  of the real part of the tangential wave number  $\text{Re } k_\tau$  assuming the wave number  $k_n$  fixed and using dispersion equation (9) for the partial electromagnetic mode with  $\omega = \omega_m$ :

$$\text{Re } \omega_m - \omega_0 = \frac{c^2 k_\tau}{\varepsilon \omega_0} \delta k_\tau = 2\beta \delta k_\tau. \quad (29)$$

Here, again  $\beta = c^2 \bar{k}_\tau / (2\varepsilon \omega_0)$ , and the reference point for  $\text{Re } k_\tau$  is selected at  $\text{Re } \omega_m = \omega_0$ . Solving equation (26) in the vicinity of the frequency  $\omega_0$  with allowance for the above said, we obtain the  $\delta k_\tau$  dependence of the polariton mode frequencies:

$$\begin{aligned} \delta\omega = & -i \frac{1}{2T_2} - i \frac{\pi}{\varepsilon} \sigma_\Sigma + \beta \delta k_\tau \\ & \pm i \left[ \left( \frac{1}{2T_2} - \frac{\pi}{\varepsilon} \sigma_\Sigma - i\beta \delta k_\tau \right)^2 + \frac{\omega_c^2 l \xi}{\varepsilon} \right]^{1/2}. \end{aligned} \quad (30)$$

This dependence coincides in its form with (23) and describes the same effects, when the coefficient  $\xi$  is replaced by  $\zeta / (2C_n)$ . These coefficients are always close in quantity and identical in the case of ideal reflection from the trap surface.

For definiteness, we will analyse different particular cases by using general expression (23). In the absence of losses ( $v_2 = 0$ ,  $R_s = 1$ ,  $\varphi_{\text{bTE}} = 0$ ), we easily find the increment in the line centre

$$\Gamma = \left( \frac{\omega_c^2 l \xi}{2\varepsilon C_n} \right)^{1/2} \sim \left( \frac{\omega_c^2 l}{2\varepsilon H} \right)^{1/2}$$

and the generation region with respect to the tangential wave numbers

$$\widetilde{\delta k_\tau^2} < 2 \frac{\omega_c^2 \omega_0^2 l \xi \varepsilon}{k_\tau^2 c^4 C_n}.$$

Taking into account the exciton polarisation and field dissipation in the case of practical interest  $\sigma_\Sigma \gg \omega_c \sqrt{l/H}$ ,  $\varepsilon T_2^{-1}$ , i.e. in the case of large losses on the emission of the modes through the side face of the trap (class D laser), the generation region is broadened:

$$\beta^2 \widetilde{\delta k_\tau^2} < \frac{\pi \sigma_\Sigma}{\varepsilon} \left( \frac{\omega_c^2 l \xi T_2}{4\pi C_n \sigma_\Sigma} - 1 \right)^{1/2},$$

and the highest increment decreases down to

$$\Gamma = -T_2^{-1} + \frac{\omega_c^2 l \xi}{4\pi \sigma_\Sigma C_n}.$$

In this case, it is easy to show that for superdimensional traps with  $D \gg \lambda$  and  $|\ln R_s| \sim 1$ , due to the inequality  $\sigma_\Sigma \omega D^2 / c^2 \gg 1$ , the imaginary part of the mode frequency always exceeds the intermode frequency interval, except a narrow vicinity of the instability threshold.

Finally, in the general case the instability condition has the form

$$\frac{\omega_c^2 T_2}{4\pi \sigma_\Sigma} \frac{l}{H} \geq \frac{C_n}{H} \frac{1}{\zeta}, \quad (31)$$

where the quantity on the right is in the order of unity. Note that this condition is similar to the instability condition in a conducting homogeneous two-level medium (see, for example, [25, 26]) and differs from the latter by the multiplier of the order of  $l/H$ , which takes into account the relative resonator volume filled with excitons.

Substituting numerical values in expression (31) gives a complete quantitative correspondence with Fig. 4. Note that the difference in the instability boundaries for  $\text{TE}_0$  and  $\text{TE}_1$  modes results from the fact that these modes have different initial wave numbers  $k_n$ ,  $k_\tau$  and, correspondingly, different parameters  $\zeta$ ,  $C_n$ , etc.

Similar results, in particular, the expression for the increment  $\Gamma$  and instability condition (31), are obtained for the TM modes by substituting

$$\begin{aligned} C_n & \rightarrow \left| \frac{\partial}{\partial k_n} \sin \varphi_{\text{TM}} \right|, \\ \zeta & \rightarrow \frac{\bar{k}_n^2 \sin(\bar{k}_n h + \varphi_{\text{bTM}}) \sin(\bar{k}_n h + \varphi_{\text{TE}})}{\bar{k}_n^2 + \bar{k}_\tau^2} \\ & \quad + \frac{\bar{k}_\tau^2 \cos(\bar{k}_n h + \varphi_{\text{bTM}}) \cos(\bar{k}_n h + \varphi_{\text{TE}})}{\bar{k}_n^2 + \bar{k}_\tau^2}. \end{aligned}$$

## 6. Instability threshold and Bose condensation

In experiment [9], the threshold density  $N_s$  corresponding to the possible onset of generation proved equal to  $\sim 10^{10} - 10^{11} \text{ cm}^{-2}$ . The squares of the cooperative frequency  $\omega_c^2 \sim 10^{26} - 10^{27} \text{ s}^{-2}$  correspond to these values (in calculating with the help of the above method with the use of the lifetime  $T_1 = 2 \text{ ns}$ ). If the polarisation relaxation time  $T_2$  is limited from above by 4 ps, which is determined by the linewidth of spontaneous emission of the excitons, and



the reflection coefficients from the side face surface of the trap  $R_s$  is estimated at 0.5 and the field absorption in the substrate is neglected, the quantity in the left-hand side of instability condition (31) will be equal to  $\sim 0.08 - 0.8$ , while the instability of the modes requires values higher than unity.

In other words, the instability of the modes should not be manifested yet in this case (which is obviously seen from Fig. 4). Nevertheless, in a real experiment, the values of  $T_1$ ,  $R_s$ , and especially of  $T_2$ , which are different from those presented above, are possible. The estimate of  $T_2$  based on the linewidth of the observed spontaneous emission is only a rough approximation from above to the real time  $T_2$  determining the polarisation relaxation time of the excitons participating in the formation of polariton modes. One can see from the presented estimates that increasing  $T_2$  by several times only is sufficient to start lasing at above exciton densities and reflection coefficients from the side faces of the traps.

Moreover, during the Bose condensation, it is natural to expect the narrowing of the exciton distribution in energies, i.e. a drastic increase in  $T_2$ , perhaps, by two – three orders of magnitude up to  $T_2 \sim T_1/2 \sim 1$  ns. Therefore, during the condensation of the excitons, the system can, at once, proceed to the unstable region and lasing will develop in the trap. In this case, the excitation of polariton modes and, hence, the appearance of predominant polarisation and spatial coherence of recombination radiation similar to those observed in papers [9–12] can indicate the condensation of the excitons. If the limiting case  $T_2 \sim T_1/2 \sim 1$  ns is indeed realised in the Bose condensation of the excitons with the density  $N_s \sim 10^{10} - 10^{11} \text{ cm}^{-2}$ , the low reflection coefficient from the side faces of the trap ( $R_s \ll 1$ ) and the reflection coefficient from the substrate  $R_b \sim 0.1$ , i.e. rather small substrate conductivity ( $|\epsilon_b| \sim 20$ ), prove sufficient for laser generation of the polariton modes. This scope of problems, including the peculiarities of broadband spontaneous and resonance scattered emission, requires further detailed investigations both theoretical and experimental.

## 7. Conclusions

The performed analytical and numerical investigation of polariton modes in the trap for dipolar excitons taking into account the polarisation relaxation and possible emission of the modes through the trap boundaries shows that some of them are high- $Q$  modes, which become unstable under conditions typical of the experiments on the Bose condensation of the excitons. Thus, the threshold observed in experiments [9–12] in the dependence of the luminescence power on the pump power and temperature approximately corresponds to the instability threshold of the polariton modes, especially if the Bose condensation of the excitons starts at these parameters.

When the instability threshold is exceeded, the modes will be in the lasing regime whose investigation and elucidation of its relation with the parameters of radiation emerging from the trap and with the properties and dynamics of formation of the exciton condensate is the subject of further studies. An important circumstance here is the finite lifetime of the excitons (from few to tens of nanoseconds) supplied by the optical pump. Due to this, the condensate is constantly renewed and metastable, which gives a unique opportunity to obtain lasing due to induced

radiation during recombination of both condensed and non-condensed excitons. This possibility allows one, obviously, to implement intracavity laser spectroscopy of different fractions of the excitons and to perform dynamic diagnostics of the Bose–Einstein condensate formation, which is an urgent problem in the field of both Bose-condensation physics and laser physics.

**Acknowledgements.** This work was supported by the Grant of the President of the Russian Federation for the State Support of the Leading Scientific Schools of the Russian Federation (Grant No. NSh-4485.2008.2) and the non-profit Dynasty Foundation.

## References

1. Pitaevskii L., Stringari S. *Bose–Einstein Condensation* (Oxford: Oxford University Press, 2003).
2. Ketterle W. *Rev. Mod. Phys.*, **74**, 1131 (2002).
3. Keldysh L.V., Kozlov A.N. *Zh. Eksp. Teor. Fiz.*, **54**, 978 (1968).
4. Berman O.L., Lozovik Yu.E., Snoko D. *Phys. Rev. B*, **77**, 155317 (2008).
5. Butov L.V. *J. Phys.: Condens. Matter*, **16**, R1577 (2004).
6. Deng H., Weihs G., Snoko D., Bloch J., Yamamoto Y. *Proc. National Academy of Sciences*, **100**, 15318 (2003).
7. Yang Sen, Hammack A.T., Fogler M.M., Butov L.V., Gossard A.C. *Phys. Rev. Lett.*, **97**, 187402 (2006); Fogler M.M., Yang Sen, Hammack A.T., Butov L.V., Gossard A.C. *Phys. Rev. B*, **78**, 035411 (2008).
8. Gorbunov A.V., Timofeev V.B. *Pis'ma Zh. Eksp. Teor. Fiz.*, **83**, 178 (2006) [*JETP Lett.*, **83**, 146 (2006)].
9. Gorbunov A.V., Timofeev V.B. *Pis'ma Zh. Eksp. Teor. Fiz.*, **84**, 390 (2006) [*JETP Lett.*, **84**, 329 (2006)].
10. Gorbunov A.V., Larionov A.V., Timofeev V.B. *Pis'ma Zh. Eksp. Teor. Fiz.*, **86**, 48 (2007) [*JETP Lett.*, **86**, 46 (2007)].
11. Timofeev V.B., Gorbunov A.V. *Phys. Stat. Sol. (c)*, **5**, 2379 (2008).
12. Timofeev V.B., Gorbunov A.V., Larionov A.V. *J. Phys.: Condens. Matter*, **19**, 295209 (2007).
13. Rapaport R., Chen Gang. *J. Phys.: Condens. Matter*, **19**, 295207 (2007).
14. Kasprzak J. et al. *Nature*, **443**, 409 (2006).
15. Snoko D. *Science*, **298**, 1368 (2002).
16. Snoko D. *Nature*, **443**, 403 (2006).
17. Balili R., Hartwell V., Snoko D., Pfeiffer L., West K. *Science*, **316**, 1007 (2002).
18. Kasprzak J., Richard M., Baas A., Deveaud B., André R., Poizat J.-Ph., Dang Le Si. *Phys. Rev. Lett.*, **100**, 067402 (2008).
19. Deng Hui, Weihs G., Santori C., Bloch J., Yamamoto Y. *Science*, **298**, 199 (2002).
20. Kavokin A., Malpuech G. *Cavity Polaritons* (Amsterdam: Elsevier, 2003).
21. Kaliteevski M.A., Brand S., Abram R.A., Kavokin A., Dang Le Si. *Phys. Rev. B*, **75**, 233309 (2007).
22. Svetlo O. *Principles of Lasers* (New York: Plenum Press, 1989; Moscow: Mir, 1990).
23. Vainshtein L.A. *Elektromagnitnye volny* (Electromagnetic Waves) (Moscow: Radio i Svyaz', 1988).
24. Khanin Ya.I. *Principles of Laser Dynamics* (Amsterdam, North-Holland: Elsevier, 1995; Moscow: Nauka. Fizmatlit, 1999).
25. Belyanin A.A., Kocharovskiy V.V., Kocharovskiy V.I. *Quantum Semiclass. Opt.*, **9**, 1 (1997).
26. Zheleznyakov V.V., Kocharovskiy V.V., Kocharovskiy V.I. *Usp. Fiz. Nauk*, **159**, 193 (1989).